Unique Role of Hot-Electron Induced Self-Heating in Determining Gate-Stack Dependent Dynamic R_{ON} of AlGaN/GaN HEMTs Under Semi-ON State

Sayak Dutta Gupta, *Member, IEEE*, Vipin Joshi, Rajarshi Roy Chaudhuri, *Graduate Student Member, IEEE*, and Mayank Shrivastava, *Senior Member, IEEE*

***Abstract*— In this work, we report a unique dependence of dynamic R_{ON} on gate-stack of AlGaN/GaN high electron mobility transistors (HEMTs) on carbon (C)-doped GaN buffer under semi-on condition. Unlike the OFF-state stress, semi-ON state stressing of the devices revealed a significantly lower dynamic R_{ON} in the Schottky HEMTs when compared to SiN_x-gated HEMTs. Detailed experiments including substrate bias dependence, electro-luminescence (EL) spectrum, and electric field analysis established electron trapping in the GaN buffer to be the source of dynamic R_{ON} in both the HEMT types. An on-the-fly thermal analysis, using thermoreflectance technique, revealed Schottky HEMTs to have a higher hot electron-induced self-heating near the field plate (FP) edge as compared to SiN_x-gated devices. The higher lattice temperature was found to result in a significantly higher electron de-trapping from the buffer traps. The higher de-trapping reduced the dynamic R_{ON} in the Schottky HEMTs as compared the SiN_x-gated devices.**

***Index Terms*— AlGaN/GaN high electron mobility transistors (HEMTs), carbon (C)-doped buffer, dynamic ON-resistance, hot electrons, self-heating, semi-ON state.**

I. Introduction

WIDE scale deployability of AlGaN/GaN high electron mobility transistors (HEMTs) for power applications is still limited, despite their superior performance. This is majorly due to the increased ON-resistance (R_{ON}) exhibited by these devices immediately after switching from high-voltage OFF-state to ON-state [1], [2], [3], [4], [5], [6], [7], [8], [9], [10]. Significant efforts have been made in the past to understand factors affecting this increase in R_{ON}, referred to as dynamic R_{ON}, upon stressing in the OFF-state. This has led to several surface passivation approaches using SiN_x [1], AlN [2], GaN cap [3], and AlTiO [4], to help suppress the dynamic R_{ON} of the devices. Besides, GaN buffer designs [7], [8], [9] have also been reported to reduce the dynamic R_{ON} of these devices. However, some recent works have highlighted that not only OFF-state stressing, but also the stress conditions applied on the devices during hard switching can significantly affect its R_{ON} [11], [12], [13], [14]. During hard switching, the device is subjected to semi-ON state conditions, wherein both high electric field and high carrier density exist simultaneously [14]. This triggers the generation of hot electrons, a major source of reliability challenges in GaN HEMTs [11], [12], [13], [14], [15], [16], [17], [18], with dynamic R_{ON} being one of the most prominent ones [11], [12], [13], [14], [15]. Indeed, several works reported a higher dynamic R_{ON} due to semi-on stressing of GaN HEMTs, as compared to OFF-state stress [11], [12], [13], [14]. Recent works have also highlighted that trapping during semi-ON state is mostly at the device surface or in AlGaN barrier, with negligible trapping in the GaN buffer [12], [13]. However, these studies are mostly limited to lower drain to source voltages ($V_{DS\text{-}Stress} \leq 50$ V). Our recent studies have highlighted that stressing the device at higher $V_{DS\text{-}Stress}$ in OFF-state can lead to significant electron trapping in buffer and result in very high dynamic R_{ON} [4], [5], [6]. Moreover, dynamic R_{ON} in these stressing conditions was found to be a function of stress time (t_{Stress}). This makes it imperative to evaluate impact of electron trapping in the GaN buffer under semi-ON state stress, as a function of $V_{DS\text{-}Stress}$ and t_{Stress}.

In this work, we report and probe a unique $V_{DS\text{-}Stress}$ and t_{Stress}-dependent dynamic R_{ON} behavior in AlGaN/GaN HEMTs on carbon (C)-doped GaN buffer under semi-on conditions, which is also a function of the gate-stack. Experiments with varying substrate bias and electro-luminescence (EL) spectrum analysis are carried out to evaluate role of trapping in the GaN buffer and on the device surface, in determining dynamic R_{ON}. Furthermore, devices with relaxed electric field near the field plate (FP) edge, using $Al_{0.5}Ti_{0.5}O_y$ surface protection [4] are tested to determine impact of electric field

Manuscript received 3 August 2022; revised 19 September 2022; accepted 2 October 2022. Date of publication 19 October 2022; date of current version 30 November 2022. This work was supported by the Department of Science and Technology (DST), Government of India, and carried out at the Indian Institute of Science, Bengaluru, under Project SP/DSTO-21-0135. The review of this article was arranged by Editor M. Hua. *(Corresponding author: Sayak Dutta Gupta.)*

The authors are with the Department of Electronic Systems Engineering, Indian Institute of Science, Bengaluru 560012, India (e-mail: sayakgupta@iisc.ac.in; mayank@iisc.ac.in).

Color versions of one or more figures in this article are available at https://doi.org/10.1109/TED.2022.3212327.

Digital Object Identifier 10.1109/TED.2022.3212327

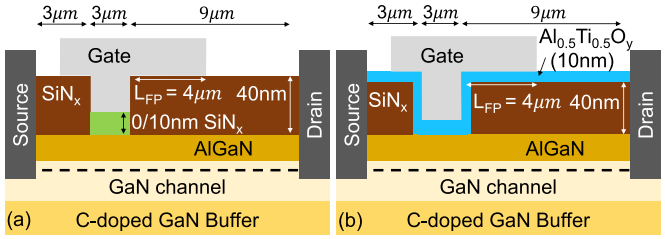

Fig. 1. Schematic of the AlGaN/GaN HEMTs fabricated for this work. (a) Schottky-gated (depicted by 0 nm SiN_x) and 10 nm SiN_x-gated HEMTs both with 40 nm SiN_x passivation. (b) $Al_{0.5}Ti_{0.5}O_y$-gated HEMTs with 10 nm $Al_{0.5}Ti_{0.5}O_y$ deposited over 40 nm SiN_x passivation.

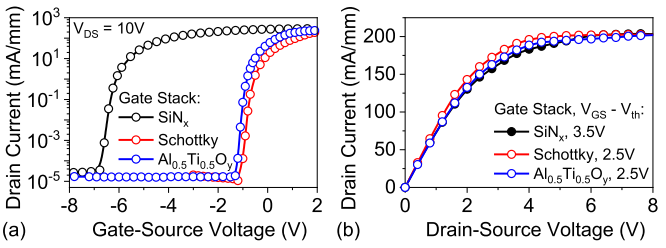

Fig. 2. (a) Transfer and (b) output characteristics of the fabricated AlGaN/GaN HEMTs. A higher gate overdrive ($V_{GS}-V_{th}$) was provided to the SiN_x-gated HEMTs to ensure similar R_{ON} as Schottky and $Al_{0.5}Ti_{0.5}O_y$-gated HEMTs, in spite of its weaker gate control.

near FP edge on trapping in GaN buffer and resulting dynamic R_{ON}. Finally, channel temperature measurements are carried out to determine any contribution of hot electron-induced self-heating in the device on its dynamic R_{ON} behavior. The electric field and hot electron-induced self-heating near the FP edge of the HEMTs, besides t_{Stress}, are established to be the factors governing the dynamic R_{ON} behavior of the HEMTs. The manuscript is organized as follows. In Section II, the device fabrication and experimental setup is described. The dynamic R_{ON} behavior of the fabricated devices is then discussed in Section III. The factors governing the dynamic R_{ON} behavior under semi-ON state stress and the related phenomenon are discussed in Sections IV and V, respectively. Finally, the work is concluded in Section VI.

II. Device Fabrication and Experimentation

AlGaN/GaN HEMTs were fabricated on a commercial grade C-doped GaN on Si epi-stack with an in-situ 40 nm SiN_x passivation. The epi-stack had a 2-D electron gas (2DEG) density of $\sim 8\times10^{12}$ cm^{-2} at the AlGaN/GaN hetero-interface. The following device variants were fabricated on the epi-stack using a well-optimized processing technology, discussed in detail in our previous works [4], [5], [19]: 1) Schottky HEMTs; 2) 10 nm SiN_x-gated HEMTs, both with 40 nm SiN_x passivation, as seen in Fig. 1(a); and 3) 10 nm $Al_{0.5}Ti_{0.5}O_y$ (AlTiO)-gated HEMTs with 40 nm SiN_x passivation + 10 nm AlTiO surface protection layer (AlTiO/SiN passivation), seen in Fig. 1(b). It is worth highlighting here that the devices were processed simultaneously using a well-optimized process to minimize process-related device variabilities. Fig. 2(a) and (b) show the transfer and output characteristics of the fabricated devices. The threshold voltage (V_{th}) of the SiN_x, Schottky, and AlTiO-gated devices was -6.5, -0.9, and -1.1 V, respectively, V_{th} being measured as the V_{GS} for $I_D = 1$ μA/mm.

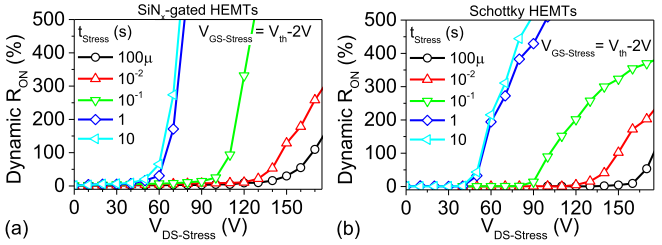

Fig. 3. Dynamic R_{ON} of (a) SiN_x-gated and (b) Schottky HEMTs with $V_{DS\text{-}Stress}$, as a function of stress time (t_{Stress}) under OFF-state stressing.

While the high-κ ($\kappa \sim 25$) and p-type nature of AlTiO resulted in V_{th} of -1.1 V for the AlTiO-gated HEMTs [4], [19], weaker channel control due to the use of 10 nm thick low-κ ($\kappa \sim 5$) SiN_x gate dielectric resulted in the significantly negative V_{th} of -6.5 V for the SiN_x-gated HEMTs [4]. Furthermore, proper surface cleaning before deposition of gate metal resulted in V_{th} of -0.9 V for the Schottky HEMTs [5]. Moreover, the HEMTs showed good ON-state and OFF-state performance with $I_{ON}/I_{OFF} \sim 10^7$.

Dynamic R_{ON} behavior of the fabricated devices was evaluated by following a measure–stress–measure–relax routine [4], [5]. The HEMT's pristine R_{ON} ($R_{Pristine}$) was first measured from inverse slope of I_D–V_{DS} for V_{DS} = 0.25–0.5 V. The devices were then stressed under semi-on condition with $V_{GS\text{-}Stress} = V_{th} + 0.3$ V, which resulted in $\sim$3 orders increase in device I_D as compared to OFF-state. The output characteristics of the HEMTs were then measured $\sim$5 ms post the stress, to evaluate its post-stress R_{ON} ($R_{Post\text{-}Stress}$). Dynamic R_{ON} of the devices was then measured as: Dynamic $R_{ON} = (R_{Post\text{-}Stress} - R_{Pristine})/R_{Pristine} \times 100$ (%). Further, $V_{DS\text{-}Stress}$ was varied from 0 to 200 V during the stressing, with t_{Stress} ranging from 100 μs to 20 s.

The dynamic R_{ON} of the HEMTs due to OFF-state stressing was also evaluated by biasing the gate at $V_{GS\text{-}Stress} = V_{th} - 2$ V, to compare the behavior with the semi-ON state dynamic R_{ON}. Moreover, given that the stressing results in degradation of the device R_{ON}, the devices were allowed a 300 s relaxation period between the $R_{Post\text{-}Stress}$ measurement and the next stress cycle to completely recover the device.

III. Dynamic R_{ON} Behavior of AlGaN/GaN HEMTs

The dynamic R_{ON} behavior of SiN_x- and Schottky-gated GaN HEMTs under OFF-state stress is shown in Fig. 3(a) and (b), respectively. The devices show presence of a t_{Stress}-dependent critical $V_{DS\text{-}Stress}$ (V_{cr}) beyond which the dynamic R_{ON} increased significantly (>25%). This dynamic R_{ON} behavior can be attributed to electron trapping in C-doping-induced traps in the GaN buffer during OFF-state stressing [4], [5]. Further, to determine how electron trapping affects dynamic R_{ON} behavior under semi-ON state stress, the SiN_x- and Schottky-gated devices were subjected to the measure–stress–measure routine in semi-ON state bias condition to extract their dynamic R_{ON}, as seen in Fig. 4(a) and (b), respectively. The figures indicate that the devices exhibit a t_{Stress}-dependent V_{cr} under semi-ON state stressing as well. The V_{cr} initially reduces with increase in t_{Stress} and remains unchanged as t_{Stress} is increased beyond

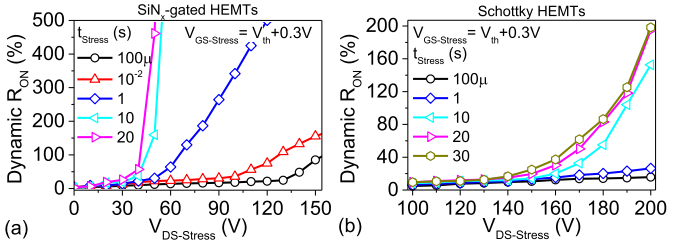

Fig. 4. Dynamic R_{ON} of (a) SiN_x-gated and (b) Schottky HEMTs with $V_{DS\text{-}Stress}$, as a function of stress time under semi-ON state stressing.

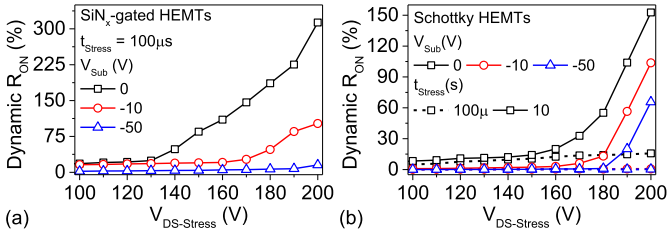

Fig. 5. Dynamic R_{ON} under semi-ON state stressing of (a) SiN_x- and (b) Schottky HEMTs with $V_{DS\text{-}Stress}$, as a function of substrate bias (V_{Sub}).

10's of seconds. However, the SiN_x-gated devices exhibit a significantly lower V_{cr} and the onset of increase in dynamic R_{ON} for lower t_{Stress} values, as compared to Schottky-gated devices. A comparison of Figs. 3 and 4 thus suggests electron trapping in C-doped GaN buffer to be a critical phenomenon determining dynamic R_{ON} behavior of the device in semi-ON state as well.

The t_{Stress} dependence of dynamic R_{ON} in SiN_x- and Schottky-gated devices under OFF and semi-ON state stressing is worth highlighting here. Fig. 3(a) and (b) show that under OFF-state stressing both SiN_x- and Schottky-gated devices show a similar t_{Stress} dependence with a minor variation in V_{cr}. On the other hand, Fig. 4 shows that while SiN_x-gated devices exhibited a V_{cr} like phenomenon for t_{Stress} as low as 100 μs, the Schottky HEMTs did not show any V_{cr} for $t_{Stress} < 10$ s. This establishes the presence of an additional phenomenon in semi-ON state, which is not observed in OFF-state, that controls dynamic R_{ON} behavior of the device. Furthermore, this additional process in semi-ON state exhibits a gate-stack dependence leading to different dynamic R_{ON} behavior of Schottky- and SiN_x-gated devices.

IV. Factors Affecting Dynamic R_{ON} under Semi-ON State

Discussions in previous section suggested the presence of electron trapping-induced V_{cr} in dynamic R_{ON} behavior of GaN HEMTs under semi-ON state stressing. Moreover, the gate-stack dependence of t_{Stress} behavior of dynamic R_{ON} in semi-ON state stressing condition suggested presence of an additional phenomenon. In this section, detailed experimentations are carried out to probe into different factors affecting V_{cr} and dynamic R_{ON} of the device under semi-ON state stressing. All measurements in this section are carried out under semi-ON state stressing unless stated otherwise.

A. Source of Dynamic R_{ON}

Dynamic R_{ON} in AlGaN/GaN HEMTs is attributed to trapping in surface and/or buffer traps [11]. To segregate the role of buffer and surface traps in determining the dynamic R_{ON} of GaN HEMTs, determination of dynamic R_{ON} behavior as a function of substrate bias (V_{Sub}) can play a critical role [4], [5]. Modification of V_{Sub} would have negligible impact on surface trapping-induced dynamic R_{ON} due to screening by the 2DEG. However, changing V_{Sub} would significantly vary carrier injection and thereby trapping in the buffer or buffer-induced dynamic R_{ON} [4], [5]. Fig. 5(a) shows the dynamic R_{ON} of the SiN_x-gated HEMTs to significantly reduce as V_{Sub} is reduced below 0 V. A similar dependence of dynamic R_{ON} on V_{Sub} is noticed for the Schottky HEMTs in Fig. 5(b). This correlation between the HEMT's dynamic R_{ON} and V_{Sub} indicates a greater role of buffer traps in the observed dynamic R_{ON} behavior.

Trapping in the gate-stack can be another source of gate-stack dependent dynamic R_{ON} in GaN HEMTs. To determine any trapping in the gate-stack, transfer characteristics of the HEMTs was measured before and after the stress cycle. The results, as shown in Fig. 6(a), depict a negligible impact of stress cycle on V_{th} of the devices. This indicates trapping to be more prominent in the access region as compared to the gate-stack of the device.

Above discussion establishes trapping in access region of the C-doped GaN buffer to be the major contributor in determining the HEMT's dynamic R_{ON} behavior. The mechanism responsible for the trapping is discussed in the next section.

B. Mechanism Responsible for Trapping

Given the role of buffer traps in the observed dynamic R_{ON} behavior, there can be two major mechanisms governing the phenomenon: 1) electron trapping [4], [5] and 2) hole emission and redistribution [10]. Electron trapping refers to the phenomenon where channel electrons injected into the C-doped GaN buffer get trapped in the buffer acceptor traps, thereby resulting in dynamic R_{ON} [5]. On the other hand, emission of holes from buffer acceptor traps near the channel/buffer interface followed by redistribution of these holes near the buffer/nucleation interface results in increase in negatively ionized buffer acceptor traps near the channel during stressing [10]. This increased negative charge near the channel results in channel depletion, leading to dynamic R_{ON}.

Substrate biasing is an effective tool in determining the dominant trapping mechanism under a given bias condition [5]. A negative V_{Sub} would oppose the injection of electrons into the GaN buffer, thereby reducing electron trapping in the GaN buffer and related dynamic R_{ON}. On the other hand, it would enhance redistribution of the holes emitted from the buffer acceptor traps to the buffer/nucleation interface, thereby increasing dynamic R_{ON} [10]. Fig. 5 shows reduction in dynamic R_{ON} of the HEMTs with negative V_{Sub}. The figure thus indicates electron trapping in the C-doped GaN buffer to be the major contributor of dynamic R_{ON} in GaN HEMTs.

In addition to substrate biasing, another way to determine electron trapping in the GaN buffer is to observe signatures of interaction of electrons with the buffer traps. Taking advantage of the fact that the device is stressed in semi-ON state,

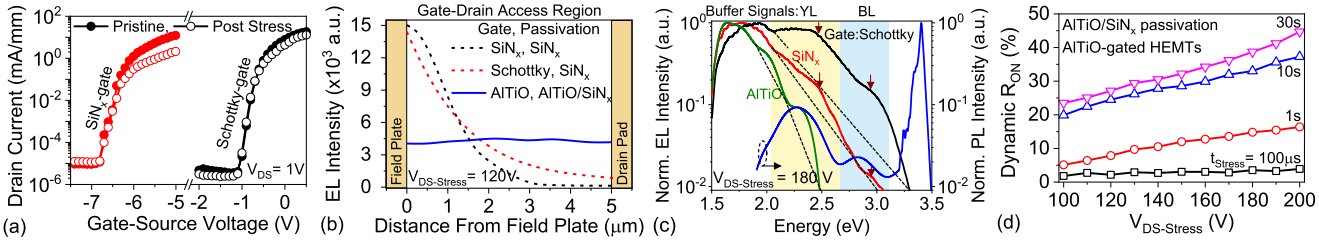

Fig. 6. (a) I_D–V_{GS} of the devices measured under pristine condition and post a semi-ON state stressing ($V_{GS\text{-}Stress} = V_{th} + 0.3$ V, $V_{DS\text{-}Stress} = 180$ V, $t_{Stress} = 1$ s). (b) EL line scans in gate–drain access region of the devices. (c) PL spectra of the GaN buffer obtained with 325 nm laser, showing the band-edge transitions, YL and BL bands. The EL spectra obtained at the FP edge of the SiN_x- and Schottky-gated HEMTs show deviation (indicated by arrows) from the Maxwellian tail (indicated by dotted lines) in the YL and BL bands. (d) Dynamic R_{ON} of the $Al_{0.5}Ti_{0.5}O_y/SiN_x$ passivated HEMTs with $V_{DS\text{-}Stress}$, as a function of t_{Stress}, under semi-ON state stressing.

EL spectrum analysis can be used to determine interaction of hot electrons with buffer traps [18]. EL line scans of SiN_x- and Schottky-gated devices depict peak EL intensity near the FP edge, as shown in Fig. 6(b). This establishes EL hot spot to be near FP edge, where EL spectrum analysis should be carried out to determine interaction of hot electrons with buffer traps. Keeping above discussion in mind, EL spectrum of SiN_x- and Schottky devices was captured near the FP edge during stressing the device in semi-ON state with a $V_{DS\text{-}Stress}$ of 180 V and $t_{Stress} > 30$ s. Such a stress condition was selected as it induced significant dynamic R_{ON} in both the devices. The results are as shown in Fig. 6(c). It shows that the EL intensity deviates from the Maxwellian tail-like features as we move toward higher energy values in the EL spectrum. This deviation is attributed to emergence of distinct peaks in the spectrum, indicated by arrows in the figure. A comparison of the EL spectra with the photoluminescence (PL) spectra of the GaN buffer indicates that these peaks correspond to the C-doping-induced yellow luminescence (YL) and blue luminescence (BL) bands [20], as seen in Fig. 6(c). The figure thus establishes interaction of hot electrons with the C-doping-induced buffer traps for both the SiN_x- and Schottky-gated HEMTs. The above experiments thus establish trapping of electrons in the GaN buffer traps to be the major source of V_{cr} and high dynamic R_{ON} observed in these devices.

C. Role of Electric Field

Discussion in the previous section established an interaction of hot electrons with buffer traps near the FP edge. To determine how this interaction affects dynamic R_{ON} behavior of the device, a relaxation in the EL intensity near the FP edge is required. To achieve this objective, devices with AlTiO surface protection over the SiN_x passivation [4], as shown in Fig. 1(b), were fabricated. Surface charge modulation due to p-type nature of AlTiO surface protection effectively relaxes EL intensity near the FP edge [4], [21], as can be seen from EL intensity plots for AlTiO/SiN surface passivated devices in Fig. 6(b). The figure shows a uniform distribution of EL intensity in the entire gate–drain access region for devices with AlTiO/SiN surface passivation. Dynamic R_{ON} of these devices is shown in Fig. 6(d). The figure shows an absence of V_{cr} like phenomenon for these devices even for a t_{Stress} of 30 s. This establishes mitigation of electron trapping in the C-doped GaN buffer by EL intensity relaxation near the FP edge. As EL intensity is a direct measure of the magnitude of electric field, this further establishes that electric field relaxation near FP edge can mitigate electron trapping and hence V_{cr} in the dynamic R_{ON} behavior of AlGaN/GaN HEMTs. The observed increase in dynamic R_{ON} values without a V_{cr} for higher values of $V_{DS\text{-}Stress}$ and t_{Stress}, as seen in Fig. 6(d), can be attributed to hole emission from buffer traps [10], or trapping of hot electrons in the surface traps [12], [13].

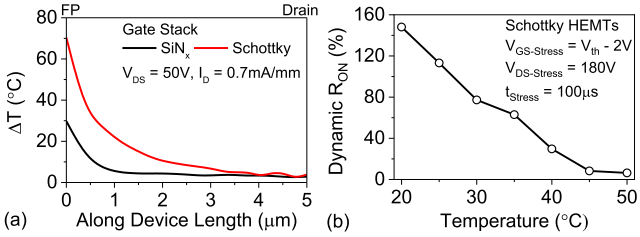

Fig. 7. (a) Average temperature (ΔT) profile of the GaN channel in the gate–drain access region of the devices, obtained using a thermo-reflectance setup. The ΔT profile was measured as increase in device temperature as compared to ambient, under semi-ON state stressing with similar dissipated power. (b) Impact of temperature on OFF-state dynamic R_{ON} of Schottky HEMTs.

D. Role of Lattice Temperature

Discussion till now has established the role of electron trapping in GaN buffer and its dependence on channel electric field in determining the dynamic R_{ON} behavior of the devices. These parameters did not show any dependence on gate-stack, thereby suggesting a gate-stack independent dynamic R_{ON} behavior. However, Fig. 4 depicts a significantly different dynamic R_{ON} behavior of the Schottky- and SiN_x-gated HEMTs. Explanation of this dependence thus needs an understanding of the impact of hot electrons on device parameters.

Apart from trapping processes, ionization of buffer acceptor traps can be affected by temperature distribution within the device. Stressing in semi-ON state can result in significant self-heating of the device due to increase in phonon population triggered by hot electron-lattice interaction [18]. This self-heating can modulate buffer trap ionization and hence will affect dynamic R_{ON} of the device. The channel temperature profile for the SiN_x- and Schottky- gated HEMTs along the gate–drain access region is measured using a thermo-reflectance setup with 365 nm noncoherent LED light source and shown in Fig. 7(a). The devices were biased in semi-ON state with similar drain current for ~5 s while

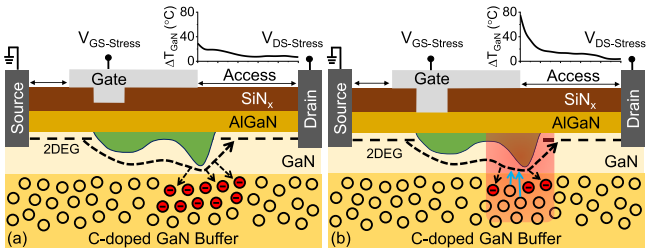

Fig. 8. Schematic showing the phenomenon governing semi-ON state stressing-induced dynamic R_{ON} in (a) SiN_x-gated and (b) Schottky HEMTs. The depletion region (electric field) in the devices near the FP edge results in injection of electrons into the GaN buffer of the HEMTs (shown by black arrows). Higher lattice temperature (shown by red window) of the Schottky HEMTs near the FP edge however results in de-trapping of carriers from buffer traps (shown by the blue arrows). This enhanced de-trapping results in lower net trapping in the GaN buffer of the Schottky devices.

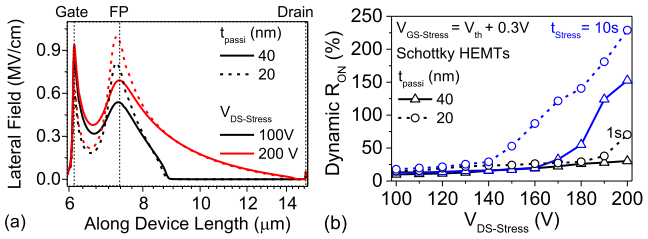

Fig. 9. (a) Lateral electric field profile in Schottky gated HEMTs, extracted using TCAD simulations, as a function of $V_{DS\text{-}Stress}$ and SiN_x passivation thickness (t_{passi}). (b) Experimentally extracted dynamic R_{ON} of Schottky HEMTs with varying t_{passi}, as a function of $V_{DS\text{-}Stress}$ and t_{Stress}.

extracting the temperature profile. The figure shows a ~2.5× higher temperature near the FP edge of the Schottky devices, as compared to the SiN_x-gated HEMTs. Higher temperature in Schottky HEMTs can be attributed to a stronger hot electron–GaN buffer interaction, as observed from Fig. 6(c). However, the phenomenon governing the observed higher temperature in Schottky HEMTs needs further investigation. Furthermore, higher temperature is known to increase hole emission [10] and should have increased dynamic R_{ON}. However, Fig. 4 shows a lower dynamic R_{ON} in Schottky HEMTs, as compared to SiN_x-gated HEMTs. This further establishes dynamic R_{ON} behavior to be not determined by hole emission.

To evaluate how temperature affects electron trapping-induced dynamic R_{ON} in Schottky devices, its dynamic R_{ON} behavior was tested at different temperatures in OFF-state. OFF-state stressing was selected here as it would induce minimum self-heating in the device due to lower currents, and also exhibits electron trapping-induced dynamic R_{ON} [5]. This allows determination of impact of temperature on electron injection and dynamic R_{ON}. Fig. 7(b) shows significant reduction in dynamic R_{ON} of the Schottky HEMTs under OFF-state stress, as device temperature is increased from 20 °C to 50 °C. Moreover, the HEMTs showed negligible dynamic R_{ON} when the device temperature was increased beyond 45 °C. This indicates a reduction in electron trapping-induced dynamic R_{ON} at higher temperature, which can be explained by thermal excitation-induced de-trapping of electrons trapped in the buffer acceptor traps.

The significantly high temperature near the FP edge of the Schottky HEMTs during semi-ON state stressing [see Fig. 7(a)] would hence result in similar de-trapping process. This reduces the dynamic R_{ON} of the devices as compared to the SiN_x-gated HEMTs, as seen in Fig. 4. The self-heating-induced de-trapping of electrons from buffer traps thus explains the gate-stack dependence of dynamic R_{ON} behavior of the devices.

V. Phenomenon Governing Dynamic R_{ON} Under Semi-ON State Stressing

Based on the above discussions, the phenomenon governing the semi-ON state stressing induced V_{cr} for dynamic R_{ON} in AlGaN/GaN HEMTs is depicted in Fig. 8. The high electric field near the FP edge of both the SiN_x-gated and Schottky HEMTs results in injection of electrons into the C-doped GaN buffer, as shown in Fig. 8(a) and (b) respectively. These electrons get trapped in the buffer traps and result in dynamic R_{ON} in the SiN_x-gated devices. However, the hot electron-induced self-heating in the channel of the Schottky HEMTs near the FP edge (where maximum trapping happens) results in increased electron de-trapping from these traps, as shown in Fig. 8(b). This enhanced de-trapping reduces the net electrons trapped in the GaN buffer and thus the dynamic R_{ON} of the Schottky HEMTs, as seen in Fig. 4.

Further, the t_{Stress} dependence of the dynamic R_{ON} behavior of the devices (see Fig. 4) can be explained as follows. An increase in dynamic R_{ON} requires substantial trapping in the GaN buffer [5]. This trapping would be determined by the number of electrons available in the buffer, probability of trapping and time available for trapping. While the electrons available in the buffer and probability of trapping is controlled by the electric field near FP edge or $V_{DS\text{-}Stress}$, t_{Stress} determines the time available for trapping. Increasing t_{Stress} thus relaxes the requirement of $V_{DS\text{-}Stress}$ needed to obtain the same concentration of ionized buffer traps necessary for exhibiting increased dynamic R_{ON} in these devices. Hence, increasing t_{Stress} reduces the V_{cr} required for high dynamic R_{ON} in the SiN_x-gated HEMTs, as seen in Fig. 4(a). Moreover, enhanced de-trapping near the FP edge of the Schottky HEMTs, due to higher hot electron-induced self-heating, reduces the net electron trapping in the C-doped GaN buffer. Thus, a higher t_{Stress} and $V_{DS\text{-}Stress}$ is required to achieve a similar concentration of ionized buffer traps so as to exhibit high dynamic R_{ON}, as seen in Fig. 4(b). Furthermore, increasing t_{Stress} reduces net traps available in the GaN buffer for electron trapping. This reduces electron trapping and can be balanced by Poole-Frenkel emission (PFE) from the ionized buffer traps at longer t_{Stress} (~few seconds) [5]. This balance of electron trapping and PFE results in the saturation of V_{cr} for t_{Stress} beyond ~10's of seconds, as seen in Fig. 4.

The dependence of dynamic R_{ON} on electric field strength at FP edge ($V_{DS\text{-}Stress}$) and t_{Stress} can be validated by comparing dynamic R_{ON} behavior of the devices with different field magnitude near the FP edge. Computational estimation of electric field of devices with different SiN_x passivation thickness (t_{passi}), as shown in Fig. 9(a), shows that this objective can be achieved by varying t_{passi}. Decreasing t_{passi} increases the electric field strength at FP edge, as seen in Fig. 9(a).

This increased electric field strength would lead to an increase in electron injection and subsequent trapping, thereby resulting in an increase in dynamic R_{ON} of the device with reduction in t_{passi}, as experimentally observed in Fig. 9(b). Moreover, Fig. 9(b) also shows a reduction in V_{cr} with reduction in t_{passi}. This dependence of dynamic R_{ON} and V_{cr} on field magnitude near FP edge validates the phenomenon proposed in Fig. 8.

VI. Conclusion

Experimentations on Schottky and SiN_x-gated AlGaN/GaN HEMTs on C-doped GaN buffer revealed a gate-stack-dependent dynamic R_{ON} behavior under semi-ON state stressing. Experiments showed a critical drain to source stress voltage beyond which dynamic R_{ON} increased significantly. However, it was observed at higher stress voltages and stress times for the Schottky HEMTs as compared to the SiN_x-gated devices. A similar critical voltage and dynamic R_{ON} behavior of both the devices under OFF-state stressing established the gate-stack dependence to be unique to semi-ON state stressing. Experiments showing reduction in dynamic R_{ON} with negative substrate bias established electron trapping in the C-doped GaN buffer to govern dynamic R_{ON} in both the devices. Moreover, interaction of hot electrons with buffer traps in EL spectra near the FP edge in both the devices established trapping to be happening near the FP edge. Thermoreflectance analysis however showed a significantly higher channel temperature near the FP edge of the Schottky HEMTs. This was attributed to self-heating induced by interaction of highly energetic hot electrons with the GaN buffer. The observed higher temperature was proposed to accelerate de-trapping from the C-doped GaN buffer and thereby reduce dynamic R_{ON}. Reduction in the dynamic R_{ON} of Schottky HEMTs under OFF-state stress (i.e., absence of channel hot electrons) at higher temperatures validated this proposal. Identical trapping due to similar electric field conditions but increased hot electron-induced self-heating and resulting de-trapping leads to a reduction in net ionized traps in the C-doped GaN buffer of the Schottky HEMTs. This results in requirement of a higher stress voltage and stress time for inducing high dynamic R_{ON} in the Schottky HEMTs, as compared to the SiN_x-gated AlGaN/GaN HEMTs, under semi-ON-state stressing conditions.

Acknowledgment

The authors would like to thank the National Nanofabrication Center (NNfC), Indian Institute of Science at Bangalore, Bengaluru, India, funded by MeitY and DST, Government of India. Sayak Dutta Gupta and Rajarshi Roy Chaudhuri would also like to thank DST INSPIRE for their fellowship.

References

[1] A. D. Koehler et al., "Impact of surface passivation on the dynamic on-resistance of proton-irradiated AlGaN/GaN HEMTs," *IEEE Electron Device Lett.*, vol. 37, no. 5, pp. 545–548, May 2016, doi: 10.1109/LED.2016.2537050.

[2] Z. Tang, S. Huang, X. Tang, B. Li, and K. J. Chen, "Influence of AlN passivation on dynamic on-resistance and electric field distribution in high-voltage AlGaN/GaN-on-Si HEMTs," *IEEE Trans. Electron Devices*, vol. 61, no. 8, pp. 2785–2792, Aug. 2014, doi: 10.1109/TED.2014.2333063.

[3] G.-Y. Lee, P.-T. Tu, and J.-I. Chyi, "Improving the off-state characteristics and dynamic on-resistance of AlInN/AlN/GaN HEMTs with a GaN cap layer," *Appl. Phys. Exp.*, vol. 8, no. 6, Jun. 2015, Art. no. 064102, doi: 10.7567/apex.8.064102.

[4] S. D. Gupta, V. Joshi, R. R. Chaudhuri, and M. Shrivastava, "Novel surface passivation scheme by using P-type AlTiO to mitigate dynamic on resistance behavior in AlGaN/GaN HEMTs—Part II," *IEEE Trans. Electron Devices*, vol. 68, no. 11, pp. 5728–5735, Nov. 2021, doi: 10.1109/TED.2021.3064531.

[5] S. D. Gupta, V. Joshi, R. R. Chaudhuri, and M. Shrivastava, "Part I: Physical insights into dynamic R_{ON} behavior and a unique time-dependent critical stress voltage in AlGaN/GaN HEMTs," *IEEE Trans. Electron Devices*, vol. 68, no. 11, pp. 5720–5727, Nov. 2021, doi: 10.1109/TED.2021.3109847.

[6] S. D. Gupta, V. Joshi, R. R. Chaudhuri, and M. Shrivastava, "Unique gate bias dependence of dynamic on-resistance in MIS-gated AlGaN/GaN HEMTs and its dependence on gate control over the 2-DEG," *IEEE Trans. Electron Devices*, vol. 69, no. 3, pp. 1608–1611, Mar. 2022, doi: 10.1109/TED.2022.3144378.

[7] G. Verzellesi et al., "Influence of buffer carbon doping on pulse and AC behavior of insulated-gate field-plated power AlGaN/GaN HEMTs," *IEEE Electron Device Lett.*, vol. 35, no. 4, pp. 443–445, Apr. 2014, doi: 10.1109/LED.2014.2304680.

[8] M. J. Uren et al., "'Leaky dielectric model for the suppression of dynamic R_{ON} in carbon-doped AlGaN/GaN HEMTs," *IEEE Trans. Electron Devices*, vol. 64, no. 7, pp. 2826–2834, Jul. 2017, doi: 10.1109/TED.2017.2706090.

[9] H.-S. Kang et al., "Suppression of current collapse in AlGaN/GaN MISHFET with carbon- doped GaN/undoped GaN multi-layered buffer structure," *Phys. Status Solidi A*, vol. 212, no. 5, pp. 1116–1121, 2015, doi: 10.1002/pssa.201431668.

[10] N. Zagni et al., "'Hole redistribution' model explaining the thermally activated R_{ON} stress/recovery transients in carbon-doped AlGaN/GaN Power MIS-HEMTs," *IEEE Trans. Electron Devices*, vol. 68, no. 2, pp. 697–703, Feb. 2021, doi: 10.1109/TED.2020.3045683.

[11] M. Wang et al., "Investigation of surface- and buffer-induced current collapse in GaN high-electron mobility transistors using a soft switched pulsed I–V measurement," *IEEE Electron Device Lett.*, vol. 35, no. 11, pp. 1094–1096, Nov. 2014, doi: 10.1109/LED.2014.2356720.

[12] M. Meneghini et al., "Trapping in GaN-based metal-insulator-semiconductor transistors: Role of high drain bias and hot electrons," *Appl. Phys. Lett.*, vol. 104, no. 14, Apr. 2014, Art. no. 143505, doi: 10.1063/1.4869680.

[13] A. Minetto et al., "Hot-electron effects in AlGaN/GaN HEMTs under semi-ON DC stress," *IEEE Trans. Electron Devices*, vol. 67, no. 11, pp. 4602–4605, Nov. 2020, doi: 10.1109/TED.2020.3025983.

[14] I. Rossetto et al., "Evidence of hot-electron effects during hard switching of AlGaN/GaN HEMTs," *IEEE Trans. Electron Devices*, vol. 64, no. 9, pp. 3734–3739, Mar. 2017, doi: 10.1109/TED.2017.2728785.

[15] I. Hwang et al., "Impact of channel hot electrons on current collapse in AlGaN/GaN HEMTs," *IEEE Electron Device Lett.*, vol. 34, no. 12, pp. 1494–1496, Dec. 2013, doi: 10.1109/LED.2013.2286173.

[16] G. Meneghesso et al., "Degradation of AlGaN/GaN HEMT devices: Role of reverse-bias and hot electron stress," *Microelectron. Eng.*, vol. 109, pp. 257–261, Sep. 2013, doi: 10.1016/j.mee.2013.03.017.

[17] Y. Puzyrev et al., "Gate bias dependence of defect-mediated hot-carrier degradation in GaN HEMTs," *IEEE Trans. Electron Devices*, vol. 61, no. 5, pp. 1316–1320, May 2014, doi: 10.1109/TED.2014.2309278.

[18] R. R. Chaudhuri, V. Joshi, S. D. Gupta, and M. Shrivastava, "On the channel hot-electron's interaction with C-doped GaN buffer and resultant gate degradation in AlGaN/GaN HEMTs," *IEEE Trans. Electron Devices*, vol. 68, no. 10, pp. 4869–4876, Oct. 2021, doi: 10.1109/TED.2021.3102469.

[19] S. D. Gupta et al., "Positive threshold voltage shift in AlGaN/GaN HEMTs and E-mode operation by $Al_xTi_{1-x}O$ based gate stack engineering," *IEEE Trans. Electron Devices*, vol. 66, no. 6, pp. 2544–2550, Jun. 2019, doi: 10.1109/TED.2019.2908960.

[20] J. L. Lyons, A. Janotti, and C. G. Van de Walle, "Effects of carbon on the electrical and optical properties of InN, GaN, and AlN," *Phys. Rev. B, Condens. Matter*, vol. 89, no. 3, Jan. 2014, Art. no. 035204, doi: 10.1103/PhysRevB.89.035204.

[21] V. Joshi, S. D. Gupta, R. R. Chaudhuri, and M. Shrivastava, "Interplay between surface and buffer traps in governing breakdown characteristics of AlGaN/GaN HEMTs—Part II," *IEEE Trans. Electron Devices*, vol. 68, no. 1, pp. 80–87, Jan. 2021, doi: 10.1109/TED.2020.3034562.